Built from Unobtanium:
an ATDM Multiband Reconfigurable Synthetic Aperture Radar Antenna

by H. Paul Shuch, Ph.D.
Vice President and Chief Technology Officer
QorTek, Inc.
1965 Lycoming Creek Road, Suite 205
Williamsport PA 17701

***Abstract* – During the previous two ESTO Conferences, the author introduced an adaptive array of microstrip antennas, the operating frequency, beam geometry and steering of which were to be accomplished by electrostatic means. QorTek has recently implemented an antenna incorporating new Advanced Tunable Dielectric Materials (ATDMs) that enable large dynamic adjustment of operating characteristics through simple application of DC tuning voltages. Although these materials are still emerging as commercially available items, we have prototyped and characterized a sixteen-element array tuned with Barium-Strontium-Titanate (BST) capacitors. Characterizing the prototype's transfer function has enabled us to tune and steer the array under software control. This technology will enable NASA to integrate multiple diverse missions into a single antenna design suitable for spacecraft or high altitude aircraft structural integration.**

I. Introduction

It has been shown at the last two ESTO Conferences [1,2] that microstrip patches, which serve well as efficient antenna elements when longitudinally excited, can be capacitively loaded to vary their resonant frequency. If variable capacitors such as varactors are used for this purpose, the antenna elements can be tuned in both frequency and phase response, permitting beam steering and pattern shaping by electronic means. For the past three years, QorTek has been exploring the use of advanced tunable dielectric materials (ATDMs) as varactor replacements, to increase the dynamic tuning range and power handling capabilities of steerable arrays of such antenna elements.

II. The SARSAD Concept

Synthetic aperture radar (SAR) antennas are commonly implemented by adjusting the phase delay of transmission lines driving individual phased array elements, so as to squint the beam in a linear or raster scan of the intended target. Digital beamforming by means of analog phase-sifters is widely used, but as array elements are added in this way, the operating frequency range is diminished significantly. In the case of pulsed SAR, the resulting bandwidth may be inadequate to support the required impulse response.

Often, antenna systems are required to operate at multiple wavelengths. An example is ground penetrating radar, where the depth of surface penetration is a function of the excitation wavelength, and vertical profiling requires that the frequency of the source to be swept. In such cases, the antenna must either be inherently broadband (with the corresponding sacrifice in gain), or it must be tuned across a range of resonant frequencies.

Electronic means exist for varying the resonant frequency of antenna elements, typically through the use of capacitive or inductive loading. Such loading is produced using either micro-electro-mechanical systems (MEMS) devices or semiconductors such as varactor (variable capacitance) diodes. Either solution implies restrictions on the operating power of the resulting tuned antenna, such that it may be appropriate for receive, but not transmit, applications.

In applications such as soil moisture or mineral distribution studies, it may prove desirable to accomplish both frequency tuning and beamforming or steering in a single antenna structure. Current SAR antennas are either pattern or frequency agile, but not both. The present project seeks to provide both functions in a single antenna, accomplishing both variation in resonant frequency (i.e., tuning) and phase adjustment (i.e., steering) through the application of new advances from the field of materials science.

Figure 1 depicts a four-patch microstrip antenna array developed by the author over the past three years, as a test-bed for steerable and frequency agile antennas employing Advanced Tunable Dielectric Materials (ATDMs) to load individual antenna elements, varying both their resonant frequency and their relative signal phase under electronic control. To facilitate rapid fabrication, testing and analysis, these antenna arrays were designed to operate at 2.4 GHz, within the FCC S-band Industrial, Scientific and Medical (ISM) frequency allocation. As this allocation coincides with a widely used license-free WiFi band, an added benefit was the ready availability of suitable test equipment from the digital telecommunications industry.

Whereas it is conventional SAR practice to vary the phase of the signals applied to each individual antenna element, QorTek has developed a unique quadrant steering concept, to greatly simplify the control electronics used to steer the antenna's beam in both azimuth and elevation. These antenna modules, along with appropriate digital control hardware and software, have been combined into a 16-element Synthetic Aperture Radar Small Array Demonstrator (SARSAD), but not without experiencing some difficulties, described herein.

Figure 1
Typical microstrip phased array antenna

[1] Shuch, H. Paul, Multiband Reconfigurable Synthetic Aperture Radar Antenna, Paper B1P1, ESTC 2004 Proceedings (CD), Palo Alto CA, June 2004.

[2] Shuch, H. Paul, Updating the Multiband Reconfigurable Synthetic Aperture Radar Antenna, Paper B5P1, ESTC 2005 Proceedings (CD), College Park MD, June 2005.

III. Advanced Tunable Dielectric Materials

The fabrication of electrically tunable variable capacitors from various ferrotunable dielectric materials is widely documented. Although other tunable dielectric substrates have been employed (and, in fact, were explored under the present contract), the most mature of these Advanced Tunable Dielectric Materials (ATDMs) at present is probably Barium Strontium Titanite (BST). Challenges to overcome in producing reliable varactor replacements from BST include temperature stability (addressed through layering of multiple stochiometries, as discussed in [2]), high-voltage breakdown issues (discussed in Section IV of the present paper), and tuning linearity (addressed in Section V herein). In addition to these difficulties, a challenge facing the present project is the lack of economical availability of the required ATDMs in production quantities.

QorTek relied upon the expertise of our colleagues in the Materials Science and Engineering department at North Carolina State University, to fabricate a quantity of electrically tunable BST capacitors for use in developing the SARSAD antenna panels. The challenge was to trade off the mutually exclusive requirements of low capacitance, wide dielectric tuning range over modest voltage extremes, and low dielectric losses at microwave frequencies.

NCSU selected an interdigital capacitor (IDC) geometry for the BST capacitors, as indicated in Figues 2 and 3. One hundred devices, representing probably the entire world's supply of such BST tuning capacitors, were fabridcated, as seen in Figure 4. Their C/V performance and dielectric losses are depicted in Figure 5.

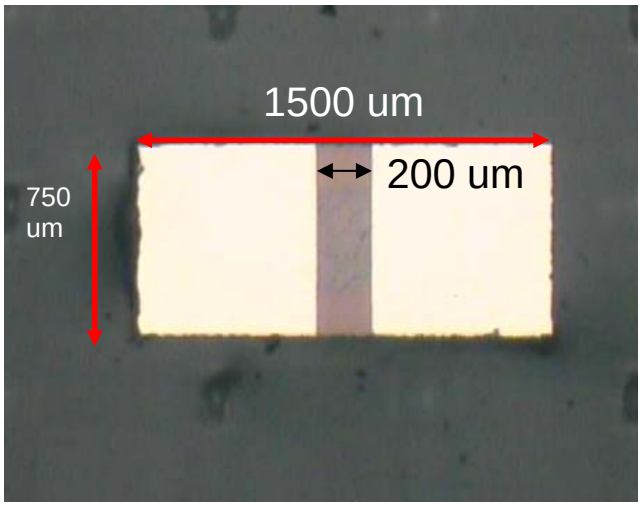

Figure 2
Critical dimensions, ATDM interdigitated capacitors

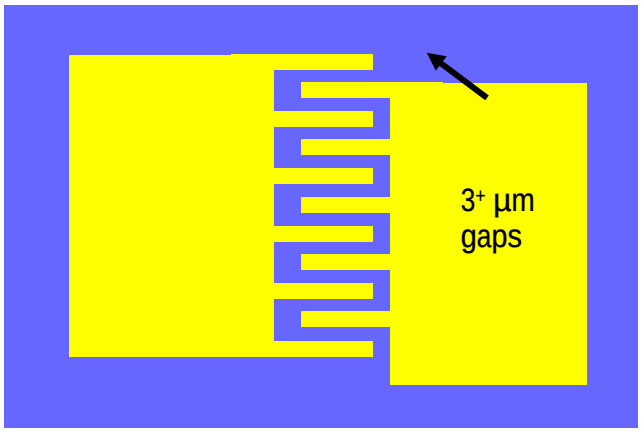

Figure 3
Gap geometry, ATDM interdigitated capacitors

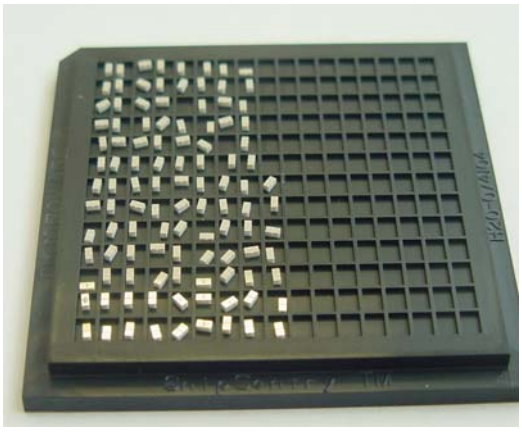

Figure 4
The world's supply of custom SARSAD BST IDCs!

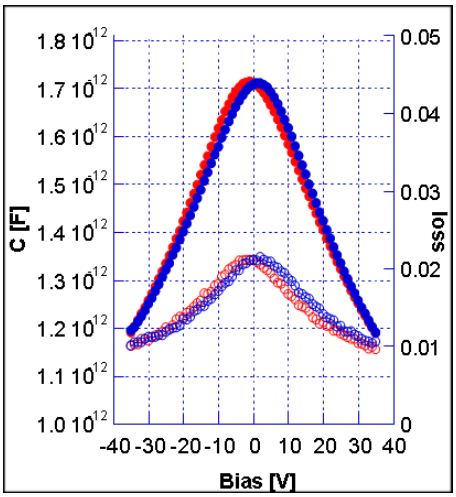

Figure 5
Measured performance, ATDM IDCs

Capacitive end-loading of microstrip patches, resulting in control of resonant frequency, as well as phase steering through detuning of the elements, was performed by affixing the IDCs to the antenna substrates with conductive silver epoxy, as indicated in Figure 6. The conductive epoxy was cured in a temperature-controlled oven at +150° C for one hour, which resulted in excellent conductivity, but generated other difficulties, as discussed in Section IV.

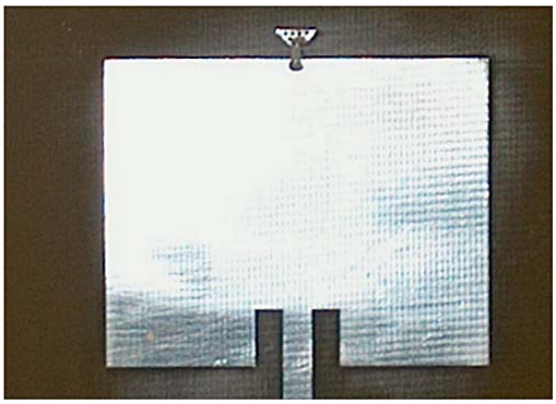

Figure 6
ATDM-loaded microstrip antenna element

IV. High Voltage Driver Circuitry

A four-channel SAR Digital Tuner developed during Year 2 of the present contract drove a varactor-tuned antenna breadboard over a 0 -12 VDC range. However, the BST capacitors used in the SARSAD require potentials of five to ten times those required of silicon epitaxial tuning diodes. Thus, it was necessary to design and fabricate a four-channel precision DC amplifier network, to interface between the tuner and the new antenna.

The circuit used to boost the bias voltages by a gain of ten is a high voltage DC amplifier seen in Figure 7. The four channel matched amplifier assembly is shown in figures 8 (circuit board) and 9 (packaged module), and interfaces directly to the existing QorTek SAR Digital Controller module through the RCA connectors depicted. The entire system is powered by the same 24 volt AC adapter brick that powers the digital tuner (described in [2]). The high voltage is achieved with an Ultravolt adjustable switching DC to DC converter. The ±15V supply comes from a DCP012415DU DC to DC converter. The male RCA plugs for the four channel input are exactly aligned to match the digital tuner box, so they can be connected directly to each other.

Evaluating the amplifier schematic, the 100k resistor to ground on the input prevents the voltage from floating when there is no input connected. The first stage of the amplifier is an operational amplifier. This is how linearity is achieved. The next stage, a complementary common base configuration (Q2 and Q3), provides most of the voltage gain. The final stage, a complementary common collector configuration (Q1 and Q4), provides some current gain and allows the amplifier to go up to the full bus voltage if needed. The two output resistors (R5 and R11) in series are current-limiting resistors for short circuit protection.

The gain of the DC amplifiers is determined by the feedback resistors (R8 and R9) and the resistor connected from ground to the non-inverting input of the op-amp (R7). Because of the two transistor stages and because the feedback is connected to the non-inverting input, even though the input is on the inverting side of the op-amp, the gain is non-inverting. Therefore, the equation to determine gain is $1+(R_{feedback}/R7)$. The amplifiers exhibit outstanding linearity, as seen in Figure 10.

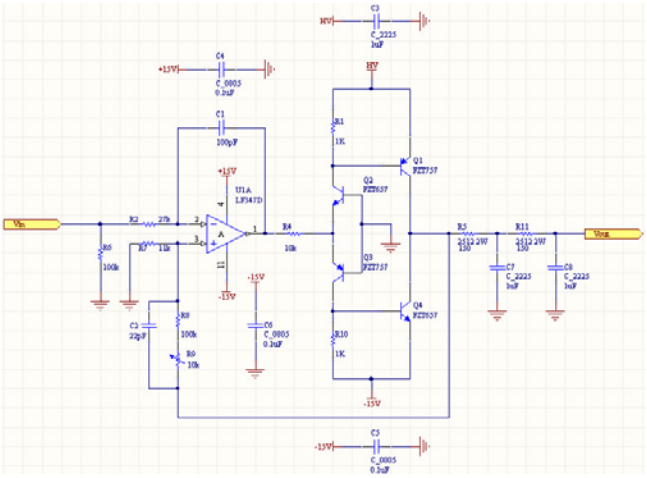

Figure 7
High-voltage driver amplifiers (schematic)

While testing the digital tuner and the amplifier along with a BST antenna panel, there was some noise observed in the system while the tuner and amplifier were connected. After looking at the output signal with an oscilloscope, it was determined that the noise, although very low in amplitude, was coming from the switching high voltage DC-DC converter. Two capacitors (C7 and C8 in Figure 7) were added to the output of each channel to create a low-pass filter to remove the noise. However, the noise could have been coming from the digital tuner, because while running a low-voltage test with just the digital tuner, noise was also evident at a detector terminating the output of the antenna when the tuner was connected. Continuing to use the filtered amplifier system should preclude a recurrence of this problem.

Figure 8
High-voltage driver amplifiers (circuit board)

Figure 9
High-voltage driver amplifiers (packaged)

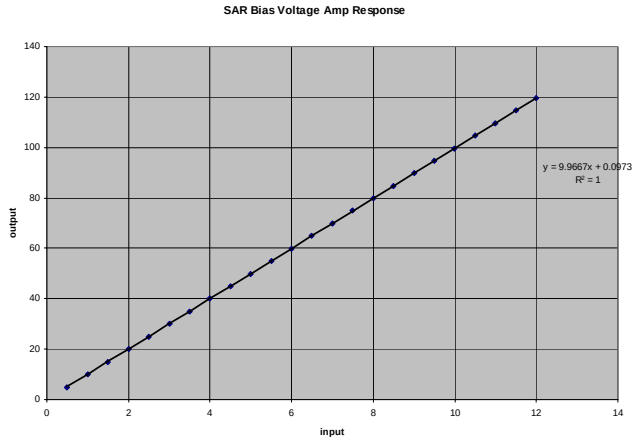

Figure 10
High-voltage driver amplifiers (response)

During testing of the first BST antenna panels, we experienced high-voltage arc-over and catastrophic breakdown of the interdigital capacitors, as seen in Figure 11. It appears that the IDCs lose their breakdown strength during the conductive epoxy cure anneal. As a temporary solution, an additional batch of IDCs was fabricated with noble metal electrodes only. Unfortunately, this increased the series resistance of the devices, and hence reduced the gain of the antennas due to dissipative losses. A more acceptable solution would be to identify a room temperature curing conductive epoxy for the IDC attach.

The gain of the high-voltage DC amplifier array is fine-tuned using the potentiometer (R9). Originally R8 was a 91k resistor, but because of resistor tolerances, a 100k ended up being used to achieve a gain of ten. Because of problems with arc-over in the BST capacitors previously noted, the gain was adjusted to five temporarily by changing R8 to a 43k ohm resistor s. Once the high-voltage arcing problem is resolved, the gain will be adjusted accordingly.

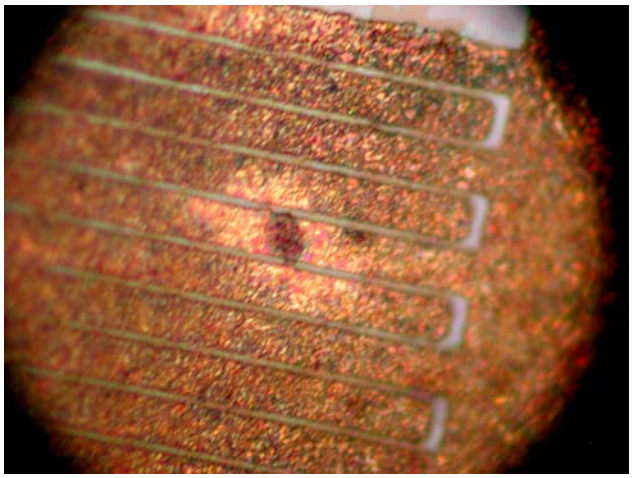

Figure 11
High-voltage damaged BST IDC

V. TUNING LINEARITY

Since our array is to be steered and tuned under digital control, it is desired to derive a transfer function for its tuning response, which we will subsequently implement in software. This SAR antenna is unique in that its tuning elements employ a ferrotunable substrate of barium-strontium-titanate (BST) developed by subcontractor Prof. Jon-Paul Maria and his graduate students at North Carolina State University. The tunable elements allow us to vary the antenna array's resonant frequency by application of DC voltages.

As a first-order approximation of an appropriate transfer function, we fit the tuning data to a linear curve, in the form $y=mx+b$. Although BST itself is touted to be a highly linear material, such is not the case for the resulting antenna, as evidenced in the tuning curve shown in Figure 12. Note the extent to which the data points diverge from the trendline. Linear regression analysis shows a correlation coefficient (R-squared) of only 0.9152.

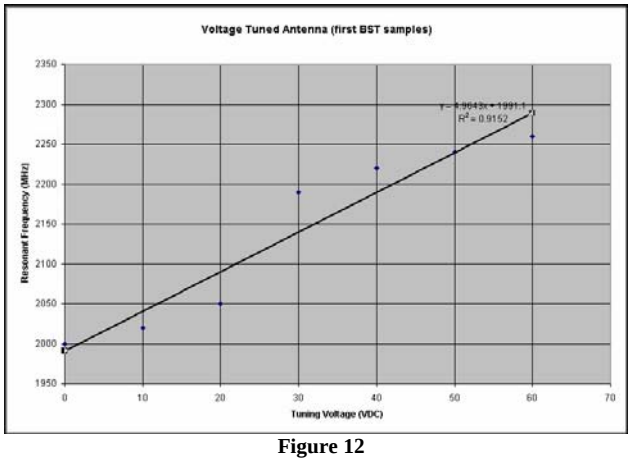

Figure 12
Frequency tuning (linear regression)

Since we desire to tune the SAR antenna in software, a more accurate transfer function is desired, calling for multivariate statistical analysis of our limited data set. Sixth-order polynomial regression produces the curve seen in Figure 13, with a perfect fit (R^2=1) to the data points. However, a word of caution is in order. Just because we can find a function which fits the available data, we shouldn't assume that function reflects reality.

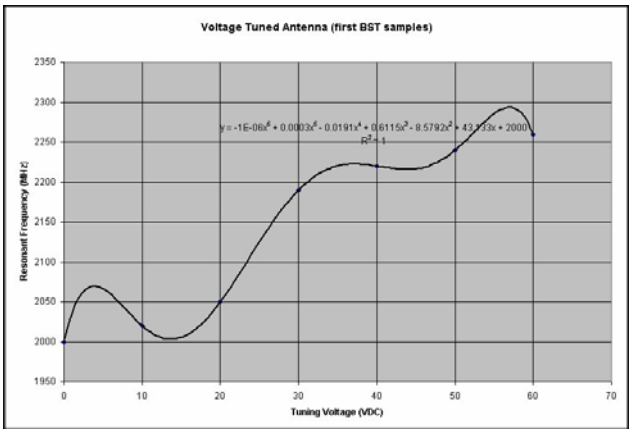

Figure 13
Frequency tuning (6th-order polynomial regression)

It is a mathematical truism that *any* n data points will *perfectly* fit an (n-1)th order polynomial equation! Consider that an n-order polynomial actually has (n+1) terms, with exponents of n through zero. (That lowest order term is just a numerical coefficient, since x^0 = 1 for any value of x.) So, if we fit an (n-1)th order polynomial to any arbitrary set of n data, the resulting curve will go precisely through all the points. At this juncture, our polynomial is not really an equation at all, but rather a lookup table expressed in polynomial form. We would expect all the points that go into a lookup table to correlate exactly with that lookup table. So, it should be no surprise that very high order polynomial curve fitting produces results that are completely accurate, and altogether useless.

In the present case, with only seven data points available, it is altogether intuitive that our correlation to a sixth-order curve shows an ideal coefficient of 1. Prudence (and the sample size rule) dictates that the number of data points being evaluated must always significantly exceed the order of the polynomial being used to characterize them.

If we take a second look at our seven data points, we conclude that, for this antenna configuration, reality is somewhat simpler than a sixth-order polynomial. Two separate and distinct linear tuning regions are evident in Figure 14.

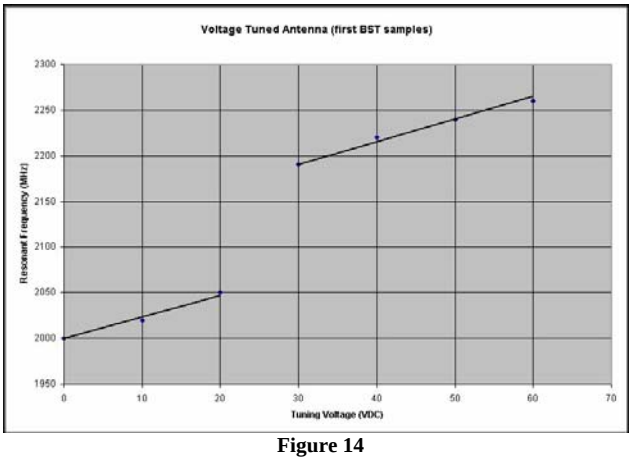

Figure 14
Frequency tuning (two distinct linear modes)

Microstrip patch antennas (such as are implemented here on a ferro-tunable dielectric substrate) can be described as cavity/slot radiators. Microwave resonant cavities can operate in multiple modes. We conclude from this Figure that our antenna is jumping between two distinct modes, each of which exhibits a relatively linear frequency response. It is our objective, when designing multiple-band antennas for actual space missions, to produce an antenna in which the various available resonant modes coincide with the actual frequency bands of interest.

For this circuit, two disjoint linear curves fit the data well. So does a sixth-order polynomial. Mathematically, either solution yields a satisfactory result. But, as far as antenna tuning is concerned, which interpretation do we consider more likely to represent reality?

The 14th Century Engish philosopher and theologian William of Ockham said it best, in his medieval rule of parsimony, which came to be known as Ockham's razor: *plurality should not be assumed without necessity*. When presented with two potential explanations for a phenomenon, the simpler of the two is most often correct.

This exercise underscores the power of graphing circuit response: it enables us to employ the Inter-Ocular Trauma Test. We accept as true those relationships which are strong enough to strike us between the eyes!

VI. Digital Control Software

Figure 15 shows a Graphical User Interface (GUI) to allow testing of the prototype array under user commands input via a laptop computer. The current GUI revision, developed under the National Instruments LabView operating system, incorporates three different graphical mechanisms for performing 4-quadrant beam steering and frequency tuning. The first, and lowest level mechanism, allows the user to individually tune each one of the quadrant tuning potentials via a graphical slider and text input box. These controls are seen in lower left hand quadrant of the GUI screenshot. The second mechanism for tuning control is in the upper left hand quadrant of the GUI screenshot. There are three slider controls that provide authority over X steering, Y steering and antenna center frequency. When the user modifies the steering and/or frequency controls, the software calculates the appropriate four tuning potentials.

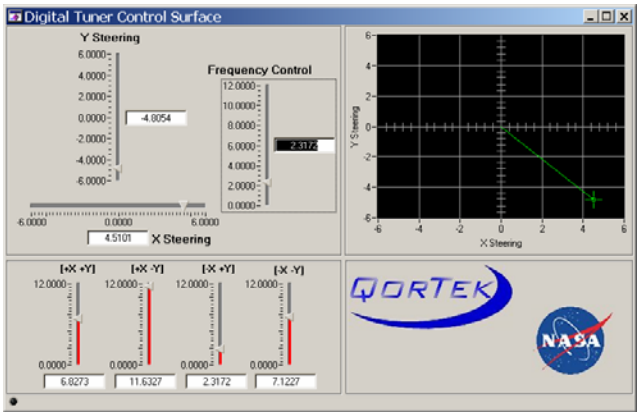

Figure 15
SARSAD GUI

The last tuning mechanism is provided via a graph/cursor control shown in the upper right section of the GUI screenshot. This control allows the user to drag a cursor about a X-Y plane to set the X and Y steering settings. It is also possible to click anywhere on the X-Y positional graph in this quadrant of the GUI, whereupon the four tuning voltages instantaneously set themselves such that the antenna array points itself to the corresponding azimuth and elevation.

Because there are three ways of controlling the tuning potentials, there is a pre-defined control priority funnel within the GUI software. A fragment of the digital controller software source code, programmed in C, illustrates this hierarchy (see Figure 16). At the lowest level of this control funnel are the 4 individual tuning potentials ([+X +Y] , [+X –Y] , [-X +Y] , [-X –Y]). All tuning changes made on the control surface map down to these four tuning potentials and are what are ultimately get transmitted to the tuning hardware via the USB interface. Changes made to the X and Y steering controls are mapped to the cursor on the graph control and then are funneled to the four tuning potentials. If the cursor is manipulated, its X and Y values are sent to the X and Y control sliders and then funneled to the four tuning potentials. As the frequency slider is manipulated, its value is mapped to the four tuning potentials as well. It is important to note that all changes made a sent to the tuning hardware in real-time. The control update loop time in the GUI algorithm is approximately 5mSec.

```
GetCtrlVal(MainCtrl,MAIN_CTRL_FSTEER,&VFSteer);
GetCtrlVal(MainCtrl,MAIN_CTRL_XSTEER,&VXSteer);
GetCtrlVal(MainCtrl,MAIN_CTRL_YSTEER,&VYSteer);

/*
To steer right, V(+X,+Y) and V(+X,-Y) increase
        V(-X,+Y) and V(-X,-Y) unchanged.

To steer left,  V(-X,+Y) and V(-X,-Y) increase
        V(+X,+Y) and V(+X,-Y) unchanged.

To steer up,    V(+X,+Y) and V(-X,+Y) increase
        V(+X,-Y) and V(-X,-Y) unchanged.

To steer down,  V(+X,-Y) and V(-X,-Y) increase
        V(+X,+Y) and V(-X,+Y) unchanged.

*/
Tpxpy = VFSteer;
Tpxmy = VFSteer;
Tmxpy = VFSteer;
Tmxmy = VFSteer;
if(VFSteer <= 6)
{
        if(VXSteer > 0)
        {
                Tpxpy += VXSteer;
                Tpxmy += VXSteer;
        }
        if(VXSteer < 0)
        {
                Tmxpy -= VXSteer;
                Tmxmy -= VXSteer;
        }
        if(VYSteer > 0)
        {
                Tpxpy += VYSteer;
                Tmxpy += VYSteer;
        }
        if(VYSteer < 0)
        {
                Tpxmy -= VYSteer;
                Tmxmy -= VYSteer;
        }
}
else
{
        if(VXSteer > 0)
        {
                Tmxpy -= VXSteer;
                Tmxmy -= VXSteer;
        }
        if(VXSteer < 0)
        {
                Tpxpy += VXSteer;
                Tpxmy += VXSteer;
        }
        if(VYSteer > 0)
        {
                Tpxmy -= VYSteer;
                Tmxmy -= VYSteer;
        }
        if(VYSteer < 0)
        {
                Tpxpy += VYSteer;
                Tmxpy += VYSteer;
        }
}
```

Figure 16
SARSAD Digital Tuner code fragment

VII. Technology Demonstrated

During the final weeks of the subject contract, all the various elements described above (multi-patch phased array antennas, ATDM tuning using BST interdigital capacitors, the SAR digital controller, high-voltage amplifier driver array, digital tuner software, and graphical user interface) were integrated into a sixteen-element Synthetic Aperture Radar Small Array Demonstrator (SARSAD), as seen in Figure 17. The SARSAD was tested first on a scalar network analyzer, to validate its frequency tuning, then on a vector network analyzer, to observe differential phase shift of the four quadrants under digital steering commands, and finally, on a compact antenna range (figure 18), to observe integrated performance as a tunable, steerable array.

Instrumentation used for array testing started with a calibrated signal source (HP 8616A microwave signal generator driving a Hawking HA16SD +6 dBi directional transmit antenna; frequency verified on a Racal Dana 9921 UHF digital frequency counter; radiated power verified on an HP 436A microwave power meter with an HP 8484 bolometer).

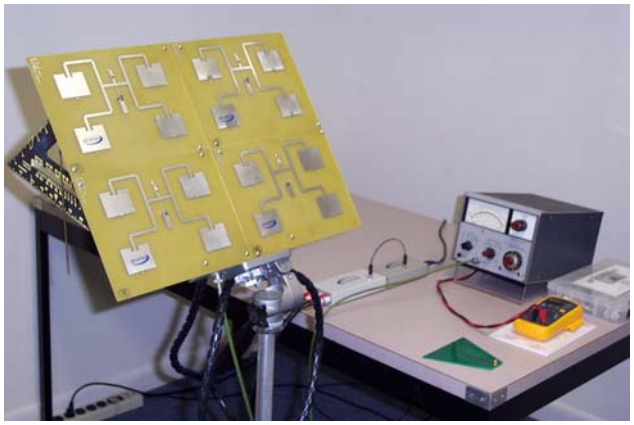

Figure 17
SARSAD gain, frequency response, and pattern tests

The antenna array under test was mounted to a Velbon VGB3 photographic tripod with a tilt and pan head. Relative azimuth was measured with a horizontal protractor, and elevation with a combination of vertical protractor and plumb bob. Received signals were measured on an HP 8559A microwave spectrum analyzer in an HP 182C display mainframe.

For both scalar and vector network analysis, we employed an HP 8754A analyzer with an HP 08754 frequency doubler. The antenna range length was calibrated for near-field, far-field, and Rayleigh zone distances, with critical tripod locations marked off on the floor with masking tape (visible in Figure 18), and corresponding free-space isotropic path losses were computed. This ensured repeatable, quantifiable measurements of the main lobe under dynamic control.

During the described testing, we encountered several difficulties. Most serious of these was a reliability problem related to high-voltage breakdown of the BST capacitors, as noted previously. During the course of validation testing, nearly three quarters of the BST capacitors failed catastrophically, limiting our ability to fully characterize the system. The reliability issue remains a challenge to be surmounted. Nevertheless, during the brief time that all four antenna quadrants were operational, it was possible to characterize the array. These measurements confirm the ability of the ATDM-tuned SARSAD to perform frequency tuning, azimuth steering, and elevation steering, simultaneously under digital control, meeting the overall objectives of the funded research.

Due to the high dielectric dissipation factor of the BST capacitors, the SARSAD antenna exhibits high loss, measured with respect to a broadband, untuned antenna. Note in Figure 19 that this loss decreases linearly with bias potential. This is consistent with the loss tangent for the BST capacitors, which can be seen to vary inversely with applied bias potential. To achieve higher TRL, it will be necessary to reduce the loss tangent of the ferrotunable dielectric by at least an order of magnitude.

Figure 18
SARSAD far-field measurements in QorTek compact antenna range

Given that the measured loss tangent for the BST capacitors employed was on the order of 10^{-2}, the reduction in antenna gain seen in Figure 19 cannot be explained by dielectric losses alone. We hypothesize that the die attach method used to integrate BST capacitors to the etched antenna panels introduces unacceptably high interface resistance. Conductive epoxy is lossy by nature, and attempts to reduce annealing temperatures (so as to avoid degradation of high voltage strength in the bulk BST) serve to aggravate this problem. Alternative methods of integrating ATDMs onto antenna panels, including direct deposition of ATDMs onto polymeric substrates should be explored in follow-on research.

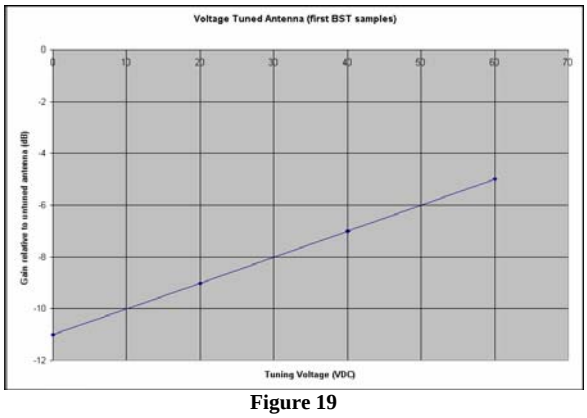

Figure 19
Excessive dielectric losses in Unobtanium make the SARSAD significantly less efficient than antennas made of conventional materials.

VIII. Applications

The research reported herein was specifically aimed at the development of instrumentation to address Strategic Objective #15 of NASA's Strategic Plan: "Explore the Sun-Earth system to understand the Sun and its effects on Earth the solar system and the space environmental conditions that will be experienced by human explorers, and demonstrate technologies that can improve future operational systems." This Strategic Objective is more fully addressed in the NASA Earth Science Technology Plan 2004, which identifies and prioritizes ESTO's program drivers. Among that document's identified Observing Systems Thrust Area Challenges is the need for "active remote sensi9ng technologies to enable atmospheric, cryospheric and Earth surface measurements." One area of observing technology need is active microwave systems for measurements of precipitation, clouds, land surface topography, and ice and snow. This implies a need for large lightweight, deployable antenna systems, which the present research attempts to address.

Several specific NASA Earth Science Technology Office programs were identified at the outset of the subject research, as representing potential candidate applications for the technology being developed herein:

- Global Topography Mapping Mission – provides high resolution, digital topography mapping (L-band SAR)
- Dual Frequency, Multi-Polarization Global Mapping SAR Mission – measuring biomass and soil moisture, providing high resolution regional-scale measurements (L and X band SAR)
- Ocean Phenomenology Mission – to study low-wind wakes and high-wind mountain waves that form in the atmosphere downwind of rugged islands (C and L-band SAR)

During the course of this research, we became aware of two additional areas of potential interest to NASA:

1. Ground Penetrating Radar applications – because penetration is a function of wavelength, it is common practice to develop vertical profiles of soil samples, ocean temperatures, etc. by varying the wavelength of an illuminating radar signal. Unfortunately, the frequency variation required for effective GPR profiling exceeds the bandwidth of most high-gain radar antenna topologies. The frequency agility of ATDM-tuned antenna arrays promises to improve GPR performance, by sweeping the resonant frequency of tunable antennas in synchronization with the radar's frequency sweep. This frequency agility has implications for future missions ranging from Earth subsurface hydrology monitoring to Mars soil analysis studies.

2. Unmanned Airborne Vehicle Synthetic Aperture Radar applications – the NASA Solid Earth Science Working Group has recommended an observational program that includes both airborne and spaceborne capabilities, as reflected in the NASA Earth Science Enterprise strategic plan. To address the airborne component of this recommendation, the UAVSAR program at NASA JPL aims to replace current SAR platforms with an instrument and platform capable of generating interferometric SAR (IFSAR) images, employing change detection techniques. The present research can lead directly to antennas appropriate to such systems. It is especially promising in the area of seismic and glacial activity monitoring. Specific potential applications include detection of earth crustal deformation leading to earthquakes, monitoring the growth and life cycle of volcanoes, and exploring the formation and flow of glaciers.

In addition to the specific ESTO missions identified above, the proposed technology offers promise in the areas of:

- Satellite Television Transmission and Reception
- Mobile wireless networking
- Aerospace Telemetry
- Remote Sensing
- Weather Monitoring
- Air Traffic Control
- Missile Defense
- Electronic Countermeasures
- Command, Control, Communications & Intelligence

QorTek has been engaged in recent discussions with EADS Deutschland GmbH, Corporate Research Centre Germany, Munich, toward the development of an antenna system based upon the present technology, to enable full duplex, multiband conformal antenna systems for installation on civil aircraft in support of broadband satellite communications links. We are currently exploring export control implications of this potential global market, specifically with respect to International Traffic in Arms Regulations (ITAR) [CFR Title 22, Chapter I, Subchapter M].

Early in the present research, SAR antenna arrays were breadboarded employing conventional steering techniques, involving analog phase shifters driving multiple untuned patch antenna elements. Varactor-tuned L-band and S-band quadrature phase shifter modules were developed for this purpose, and several such units were fabricated to support early antenna testing. Although we ultimately abandoned this legacy technology solution, in favor of ATDM-tunable microstrip patch antenna elements, QorTek has introduced the interim phase shifter deesign as a commercial product. Full specification sheets for our Model PS-1420 and PS-2400 Phase Shifters may be found under the Products section of the QorTek website, www.qortek.com. We are currently exploring the feasibility of upgrading their semiconductor tuning elements to ATDM varactor replacements, to improve power handling capabilities and dynamic phase tuning range.

IX. Conclusions

The combination of advanced microstrip patch antenna designs, quadrant steering and tuning architecture, and newly emerging electrically tunable materials promises to enable the development of large-scale, flexible, steerable and frequency-agile antenna arrays, for use in aperture synthesis, scanning radar, adaptive telecommunications, and a host of related aerospace and commercial applications. During the final year of a three-year ESTO Advanced Components Technology (ACT) contract, QorTek integrated the various elements of the design into a Synthetic Aperture Radar Small Antenna Demonstrator (SARSAD), achieving Technology Readiness Level 4. Issues to be addressed in future research, before a higher TRL can be achieved, include: excessive dielectric losses resulting in compromised antenna gain, high-voltage breakdown of the ATDM IDCs, and the lack of availability of the required advanced dielectric materials in production quantities and at reasonable cost. The key required material is indeed still Unobtanium!

X. Acknowledgments

The research described herein was performed under NASA ESTO contract NAS5-03014. QorTek thanks technical representative Janice Buckner for her support, and acknowledges the contributions and assistance of our co-investigators: Prof. Susan Trolier-McKinstry of MRL, Pennsylvania State University, and Dr. Jon-Paul Maria of MSE, North Carolina State University. The author especially wishes to acknowledge the many helpful suggestions received from Dr. Daniel D. Evans of Aerospace Corporation, the NASA Advanced Component Technology (ACT) Program external reviewer on the recently concluded contract.